GRID-SIZE EFFECTS ON SURFACE RUNOFF MODELING

By D. K. Molnár[1] and P. Y. Julien,[2] Member, ASCE

ABSTRACT: The effects of grid-cell size on surface runoff modeling using a distributed hydrologic model are examined. The raster-based hydrologic CASC2D model is applied to two watersheds in northern Mississippi. Observed streamflow for Goodwin Creek (21 km^2) is used in calibrating the model's infiltration, runoff, and routing parameters. The results are extended to Hickahala-Senatobia (560 km^2), which has similar physical characteristics. The applicability of CASC2D in simulating rainfall-runoff processes is tested using square grid-cell sizes ranging from 127 to 914 m. Event-based simulation results indicate that coarser grid-cell resolutions can be used in rainfall-runoff simulations as long as parameters are appropriately calibrated. It is demonstrated that the primary effect of increasing grid-cell size on simulation parameters is to require an increase in overland and channel roughness coefficients. The concept of a watershed time-to-equilibrium is used in evaluating the runoff response of overland and channel cells. At different grid-cell sizes, raster maps generated within a GRASS GIS environment provide information regarding the spatial distribution of drainage area, time-to-equilibrium, and equilibrium discharge on Goodwin Creek and Hickahala-Senatobia. It is shown that at increasing grid-cell size, the statistical distribution of drainage areas associated with overland cells is significantly increased, while the statistical distribution of drainage areas associated with channel cells is hardly affected by grid-cell size. It is also demonstrated that flow on overland cells is more sensitive to changes in grid-cell size than is channel flow. Since channel flow dominates the shape of the hydrograph in large watersheds, the results indicate that coarse grid sizes can be used for rainfall-runoff simulations on large watersheds. The results also indicate that coarser grid sizes will be more appropriate when simulating events of high intensity or of long duration.

INTRODUCTION

Hydrological models have been developed to improve our understanding of surface runoff generated from complex watersheds. Ideally, surface runoff models should capture the essence of the physical controls of soil, vegetation, and topography on runoff production. A variety of surface runoff models are available and these models are commonly classified as either lumped-parameter models or distributed-parameter models.

Lumped-parameter models integrate watershed characteristics over a given area, neglecting heterogeneity within the area and thus resulting in simplified runoff conditions. A concern regarding lumped-parameter models is the difficulty in obtaining a single representative value of a spatially variable parameter that would lead to an accurate prediction of the mean watershed response. In addition, the problem with using measured parameter values for physically based models is that the scales at which measurements are performed are typically too small to enable incorporation of spatial variability into the models (Dunne 1982; James and Burges 1982; Beven 1983; Wood 1983).

Distributed-parameter models were developed to represent the variability in physical watershed characteristics. The use of distributed models is complicated by the need to establish an appropriate spatial scale to be used in characterizing watershed conditions such as topography, drainage density, degree of soil saturation, geomorphology, and rainfall properties. The challenge in applying distributed-parameter models to large watersheds is to determine a scale at which spatial variability can be neglected, with average characteristics of a given area providing sufficient information for accurate modeling of basin runoff generation. In support of distributed models, Geographic Information Systems (GIS) provide a unique environment that increases the potential for describing spatial variability. Distributed parameter hydrological models are typically structured such that it is advantageous to use the data currently available in GIS format. GIS technology can be used in preparing appropriate input files for the models. Advances in computer technology have made it possible to efficiently handle large amounts of data, increasing the feasibility of simulating runoff generation on large watersheds.

In an attempt to characterize runoff generation at different scales, a concept that has gained a great deal of attention is the concept of a representative elementary area (REA). Wood et al. (1988) first defined areas of similar hydrologic response as REAs, based on the theory that runoff generation is a multiscale phenomenon with different length scales characterizing soil, topography, and rainfall variability. By definition, the REA must be a length scale larger than the length scale characteristic of rapidly varying components of the hydrological response, yet smaller than the length scale of slowly varying components. The basis of the REA is that when variability is integrated over a large enough area, the effects of small-scale variability are attenuated (Sivapalan et al. 1987; Wood et al. 1988, 1990).

Dimensional analysis and similarity concepts can also be used to understand the nature of watershed runoff generation and its relation to watershed characteristics. A case in point, time-to-equilibrium has been used in describing the hydraulic response of a watershed-to-rainfall. Time-to-equilibrium is affected by spatial variability in such watershed characteristics as overland slope, roughness coefficient, and soil types, and is also affected by such rainfall properties as duration and intensity. Numerous studies have been performed using the concept of a watershed-time-to-equilibrium (Lighthill and Whitham 1955; Henderson and Wooding 1964; Agiralioglu 1984, 1988; Wooding 1965a,b, 1966; Woolhiser and Goodrich 1988; Julien and Moglen 1990; Ogden 1992; Ogden et al. 1995; Saghafian and Julien 1995; Molnár 1997). In earlier research, the relationship between time-to-equilibrium, watershed characteristics, and rainfall properties for well-defined, simple geometries were analytically derived. More recent studies have looked at applying the concept of time-to-equilibrium to specific watersheds. The effects of spatial variability on time-to-equilibrium can be evaluated in the context of raster-based runoff models, for which physical characteristics are defined on a grid cell by

[1]Postdoctoral Fellow, Dept. of Civ. Engrg., Engineering Research Ctr., Colorado State Univ., Fort Collins, CO 80523. E-mail: pierre@engr.colostate.edu

[2]Prof., Dept. of Civ. Engrg., Engineering Research Ctr., Colorado State Univ., Fort Collins, CO.

Note. Discussion open until June 1, 2000. To extend the closing date one month, a written request must be filed with the ASCE Manager of Journals. The manuscript for this paper was submitted for review and possible publication on February 3, 1998. This paper is part of the ***Journal of Hydrologic Engineering***, Vol. 5, No. 1, January, 2000. ©ASCE, ISSN 1084-0699/00/0001-0008–0016/$8.00 + $.50 per page. Paper No. 17512.

grid cell basis. The size of the grid cell used in the model will affect the overall representation of variability. In their analysis of 1D systems, Julien and Moglen (1990) found that the time-to-equilibrium of spatially varied systems can be approximated by using spatially averaged values of hydrologic parameters. They defined a length scale at which spatial variability of watershed characteristics does not have a significant effect on runoff. They concluded that it should be possible to analyze extreme events (high intensity, long duration) with larger grid-cell sizes, as long as the grids have a runoff length shorter than the equilibrium length scale.

OBJECTIVES

The objective of this study is to examine the effects of grid-cell size on surface runoff calculations using the distributed hydrologic model CASC2D. The effects of the spatial variability of watershed characteristics and rainfall properties on simulated discharge, time-to-equilibrium, drainage area, and equilibrium discharge will be examined by simulating runoff conditions using a range of grid-cell sizes. Event-based simulations on Goodwin Creek (21 km^2) allow for the calibration of the model at different grid sizes and will provide information on the effects of grid-cell size on the reproduction of rainfall-runoff processes. Hypothetical simulations on Goodwin Creek and Hickahala-Senatobia (560 km^2), based on the concept of a watershed time-to-equilibrium, will provide information on the basinwide effects of grid-cell size on equilibrium conditions.

With current advances in GIS technology, watershed input data is becoming readily available at grid-cell sizes as fine as 30 m. Yet in modeling surface runoff with the CASC2D model, the use of larger grid-cell sizes is examined because these require less input data and less computation time, and can therefore be used in simulations on large watersheds. An improved understanding of the role of spatial heterogeneity on the simulation of runoff generation will make it possible to (1) use coarser grid cells in distributed models, and (2) extend the applicability of hydrological models to large watersheds (over 500 km^2). An appropriate scale for runoff simulations on large watersheds will be one that preserves the essential characteristics governing hydrologic, hydraulic, and geomorphic processes, but for which data requirements and computation time are reduced.

CASC2D RAINFALL-RUNOFF MODEL

CASC2D is a physically based, distributed watershed model that simulates the hydrologic response of a watershed subject to spatially and temporally varied rainfall. The major components of CASC2D are distributed precipitation, interception, infiltration, and diffusive wave runoff routing. Once interception and infiltration have been subtracted from rainfall precipitation, excess rainfall generates surface runoff. The excess rainfall is then routed as overland flow, based on a 2D explicit finite-difference (FD) technique. The overland flow direction is determined by the friction slope, which is computed as a function of bed slope and flow depth. Overland flow is routed orthogonally. Once overland flow reaches a channel cell, it is routed as channel flow, based on a 1D FD technique.

As described by Julien et al. (1995), the model has been formulated using the Saint-Venant equations of continuity and momentum to describe the mechanics of both overland flow and channel flow. The diffusive wave approximation is used as a simplified form of the Saint-Venant momentum equation. The continuity and momentum equations are applied by superimposing a square grid mesh on the watershed. A numerical solution is evaluated for individual grid cells. Rainfall intensity, soil characteristics, and watershed characteristics are assumed constant within each grid cell but vary from one cell to another. The raster-based structure of the model accommodates such variations in watershed characteristics as slope, surface roughness, width of the runoff plane, soil characteristics, and the spatial and temporal distribution of rainfall.

The CASC2D model has been successfully applied to basins less than 50 km^2, using grid-cell sizes ranging from 150 to 400 m (Saghafian 1992; Ogden 1992; Doe and Saghafian 1992; Johnson 1993; Ogden and Julien 1994; Saghafian et al. 1995; Ogden et al. 1995; and Molnár 1997). Physical processes governing rainfall-runoff generation on overland cells are described using five parameters: S_d, K_s, H_f, M_d, and n_{ol}. The parameter governing channel flow is n_{chan}. Detention storage S_d represents water that is retained by leaves or in depressions, and accumulates before overland runoff occurs. Infiltration rates are calculated using the Green and Ampt infiltration scheme, requiring the following soil parameters: saturated hydraulic conductivity K_s, capillary pressure head H_f, and initial soil moisture deficit M_d. Overland discharge rates are evaluated as a function of the overland Manning roughness coefficient n_{ol}. Runoff rates in the channel network are evaluated as a function of the channel roughness coefficient n_{chan}. Rain gauge or radar data is used as rainfall input to the model. At each time step, rainfall rates on individual grid cells are determined by interpolation. The model output includes runoff hydrographs and flow depth maps.

WATERSHED TIME TO EQUILIBRIUM

The hydraulic response of a watershed to rainfall can be described using the concept of a watershed time-to-equilibrium T_e, defined as the wave travel time from the point where a raindrop falls to the ground until it reaches the outlet of the basin. The time-to-equilibrium is evaluated as a function of watershed physical and geometrical properties, and depends on storm characteristics. Woolhiser (1975, 1977) has described in great detail the concept of complete equilibrium hydrographs, using the watershed time-to-equilibrium as a delineating parameter.

For one-dimensional flow on rectangular plots, the time-to-equilibrium is obtained from the Saint-Venant equations and the Manning resistance equation (Woolhiser 1977), as

$$T_e = \left(\frac{nL}{i^{2/3} S^{1/2}}\right)^{3/5} \tag{1}$$

where T_e = time-to-equilibrium; i = rainfall intensity; n = Manning roughness coefficient; S = runoff slope; and L = runoff length.

Steady state is achieved when rainfall duration exceeds the time-to-equilibrium, when the output of the system (runoff) is equal to the input to the system (rainfall). The nature of the surface runoff hydrograph, under uniform rainfall conditions, thus depends on the rainfall duration (T_r). Assuming impervious conditions, if the rainfall duration is longer than the time required to reach equilibrium ($T_r/T_e > 1$), then complete equilibrium occurs. Under equilibrium conditions, surface runoff increases linearly with excess rainfall intensity, warranting the use of linear methods such as the unit hydrograph (UH) and the instantaneous unit hydrograph (IUH) in modeling rainfall-runoff processes. If the rainfall duration is less than the time required to reach equilibrium ($T_r/T_e < 1$), then partial equilibrium conditions exist. Under partial equilibrium conditions, the routing relationship is nonlinear and must be modeled using nonlinear methods.

Extending the concept to distributed modeling, under equilibrium conditions peak discharge is constant, and the grid-cell size used in raster-based models will not affect runoff rates. Accordingly, equilibrium discharge should not be influenced

by the spatial variability of physical grid characteristics. In contrast, when partial equilibrium conditions exist, grid-cell size should influence the rainfall-runoff conditions because of the nonlinear response of the watershed to rainfall intensity.

MODEL CALIBRATION

The CASC2D model was calibration on Goodwin Creek, a 21 km^2 watershed located in northwestern Mississippi. The creek is a tributary of Long Creek, which flows into the Yacona River, one of the main tributaries of the Yazoo River. The watershed climate is humid. Elevations range from 71 to 128 m above sea level. In overland regions, 50% of the basin has a slope less than 0.02 and 15% of the regions have slopes greater than 0.03. Land-use types are described as cultivated areas (13%) or as idle land (87%), which includes pasture and forest. The two dominant soil types are silt loam and fine sandy loam.

Goodwin Creek is an experimental basin monitored by the National Sedimentation Laboratory of the Agricultural Research Service (ARS), located in Oxford, Mississippi (Blackmarr 1995). Watershed data for runoff simulations on Goodwin Creek were obtained primarily through the U.S. Corps of Engineers Waterways Experiment Station, where CASC2D has previously been applied (Johnson 1993; Johnson et al. 1993). Input data in the form of raster maps include a digital elevation model (DEM), a soil type map, and a land-use map. Initial values of capillary pressure and hydraulic conductivity were estimated from tables of Green-Ampt parameters based on soil texture (Rawls et al. 1983). Initial estimates of overland roughness coefficients were determined from the land-use map (Johnson 1993). Channel data for Goodwin Creek include width, depth, and roughness coefficients for individual stream segments. The location of the channel was determined based on a digital elevation map, and assuming a threshold of approximately 0.5 km^2.

Over 10 years of rainfall and runoff data are currently available for the watershed. Instrumentation consists of 17 raingauges and 14 streamgauges. During high intensity rainstorms, precipitation measurements are available every minute. Outlet discharge and discharge at subbasin gauges are also available at frequent intervals during rainfall events. Based on previous simulation studies done on Goodwin Creek (Johnson 1993), three rainfall-runoff events were selected for analysis (see Molnár 1997 for additional events). Conditions for the three events are summarized in Table 1. Events 1, 2, and 3 lasted approximately 3.5, 6, and 24 h, respectively. The largest volume of rain fell during event 3, and the smallest volume of rain fell during event 2. A final distinction is that the initial soil moisture conditions differed: during the week before the events, event 1 was preceded by 2.5 mm of rain, event 2 was preceded by 10.2 mm of precipitation, and event 3 was preceded by 76 mm of precipitation.

The CASC2D model was manually calibrated using events 1 and 2. The objective of the calibration was to obtain a best fit between simulated and observed discharges, with the intent of reproducing as closely as possible the peak discharge, the time to peak, and the total volume (in that order). The objective function was to simulate the peak discharge to within 10% and the time to peak to within 15% (or less than 1 h). In these simulations, CASC2D is used as a single-event model, and initial conditions represented by the soil moisture and detention storage parameters may vary. In the course of model calibration using event 1, the parameters representing soil moisture deficit M_d and detention storage S_d were determined from rainfall conditions prior to the event. When the soil is saturated, overland runoff occurs much more rapidly, particularly when events have high rainfall intensities. Since the antecedent moisture conditions of event 1 differed from those of the other two events, the model was also calibrated using event 2 and these parameters were used to validate the model with the third event.

TABLE 1. Goodwin Creek Rainfall Events

Event number (1)	Rainfall duration (2)	Rainfall during week preceding event (3)	Average rainfall rate (4)	Rainfall volume (5)
Event 1	211 min	2.5 mm	20.60 mm/h	1,503,472 m^3
Event 2	361 min	10.2 mm	5.69 mm/h	711,970 m^3
Event 3	1,869 min	76 mm	4.72 mm/h	2,865,181 m^3

EFFECTS OF GRID-CELL SIZE ON SURFACE RUNOFF SIMULATIONS

The original raster data was obtained at a 127 m resolution. Two additional grid-cell sizes, 254 m and 380 m, were selected for the analysis. Input raster data corresponding to larger grid-cell sizes were obtained within the Geographical Resources Analysis Support System (GRASS) GIS environment. In GRASS (*Grass 4.1* 1993), when a coarser grid mesh is overlain on the original raster data, the value nearest to the center of the cell is selected as the value corresponding to the larger cell size. This method eliminates bias due to averaging and is more representative of the GIS data obtained for larger watersheds, where only coarse grid cell data is available.

GRASS GIS capabilities were used in evaluating the effects of increasing grid-cell size on the representation of basin area, the number of channel cells, the number of overland cells, and drainage density. As seen in Table 2, data aggregation to larger grid-cell sizes affected the representation of certain watershed characteristics. As grid-cell size increases, the changes are as follows: (1) The obvious reduction in total number of grid cells leads to a significant decrease in computation time for surface runoff simulations, since model computations are performed on each cell at every time step; (2) the ratio of channel cells to the total number of cells increases, increasing the importance of channel flow routing as compared to overland flow routing; and (3) the drainage density evaluated as the ratio of the total channel length to the drainage area decreases, affecting the relative contributions of overland flow and channel flow.

For modeling purposes, the channel network has been divided into links, each of which is assigned a specific channel width, depth, and roughness coefficient. The total length of the channel network is shortened as a result of increasing grid-cell size, since the stream length is assumed to be equal to the cell length within each channel node. A shortened stream network would imply steeper channel slopes. In order to maintain similar channel routing conditions at increasing grid-cell sizes, channel bed elevations have been defined such that channel slopes are constant at all three grid resolutions. The analysis of topographic maps corresponding to increased grid-cell sizes indicates that upland slopes decrease as grid-cell size is increased. As a result of data aggregation at larger grid-cell sizes,

TABLE 2. Goodwin Creek Watershed Characteristics at Increasing Grid-Cell Size

Characteristic (1)	127 m (2)	254 m (3)	380 m (4)
Drainage area (km^2)	20.74	20.71	20.26
Total number of grid cells	1,290	322	140
Number of channel cells	212	101	61
Ratio of channel cells to total cells (%)	16.4	31.4	43.6
Ratio of overland cells to total cells (%)	83.6	68.6	56.4
Total length of channel (km)	26.9	25.4	23.2
Drainage density (km^{-1})	1.30	1.24	1.15

terrain information is lost. These changes will have an impact on upland runoff rates, which are evaluated as a function of friction slope S_f, itself a function of the bed slope S_0 through the momentum equation. Although initial estimates of overland roughness coefficients differed as a function of land-use types, it was found that spatial variability in roughness in upland areas had little effect on the simulated outlet hydrograph and that a single roughness value could be used to represent upland conditions. Similarly it was found that a single channel roughness coefficient could be used to represent conditions in the stream network.

Model calibration for event 1 required different input parameters at each grid resolution for the best possible fit between simulated and observed outlet hydrographs. The hydrograph results from the calibration runs at grid-cell sizes 127, 254, and 380 m are presented in Fig. 1(a). The calibration parameters resulting in the best fit of simulated-to-observed outlet discharge for event 1 at all three resolutions are summarized in Table 3. The observed peak discharge was reproduced to within 6% and the time-to-peak to within 15%. The parameters affected by increasing grid-cell size are overland roughness n_{ol}, channel roughness n_{chan}, soil moisture deficit M_d, and capillary pressure H_f. The most significant changes are made to the overland roughness coefficient n_{ol}, which nearly doubles from 0.08 to 0.15 as grid-cell size increases. Having calibrated the model to outlet conditions, a simulated subbasin hydrograph was evaluated for comparison with the observed hydrograph. Gauge 3 was used, with a drainage area of 8.78 km^2. The gauge is located in the upper part of the watershed, on the main channel network. At the subbasin level, channel routing is expected to play less of a role, whereas upland processes are expected to become more important. The effects of grid-cell size on overland processes can thus be examined. Fig. 1(b) summarizes the results at increasing grid-cell size. The coarser grid sizes simulate lower runoff rates and earlier times-to-peak.

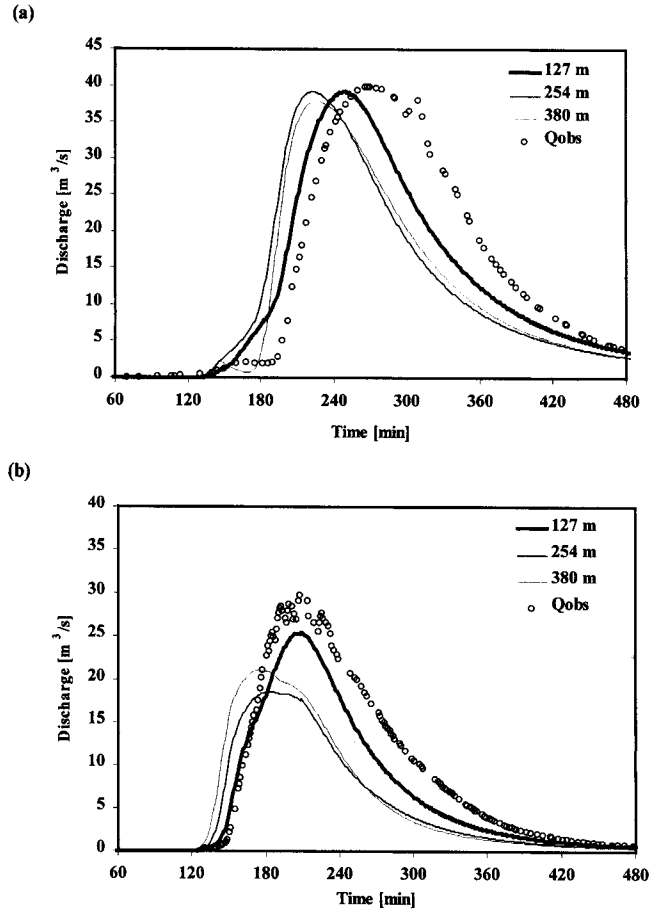

FIG. 1. Goodwin Creek Hydrographs for Event 1: (a) at Outlet; (b) at Gauge 3

TABLE 3. Calibration Parameters for Event 1

Parameter (1)	127 m (2)	254 m (3)	380 m (4)
Overland detention storage S_d (m)	0.015	0.015	0.015
Overland roughness n_{ol}	0.08	0.09	0.15
Silt loam: K_s (m/s)	1.30E-06	1.30E-06	1.30E-06
Silt loam: H_f (m)	0.16	0.16	0.1668
Silt loam: M_d	0.08	0.1	0.1
Fine sandy loam: K_s (m/s)	2.20E-06	2.20E-06	2.50E-06
Fine sandy loam: H_f (m)	0.08	0.08	0.080
Fine sandy loam: M_d	0.08	0.1	0.1
Channel roughness n_{ch}	0.037	0.037	0.04

Calibrating the model to event 2 required changing the parameters representing infiltration conditions and detention storage. Again, the objective of the calibration was to match the simulated peak discharge and the time-to-peak to the observed values. The final results from the calibration at the outlet are plotted in Fig. 2(a). As shown in Table 4, the calibrated parameter set from event 2 differed from the calibrated parameter set from event 1 (Table 3). Significant differences are noticeable in the soil parameters K_s, H_f, M_d, and the detention storage S_d. These results suggest that antecedent moisture conditions have an effect on infiltration and detention storage. Yet, as seen in Table 4, the soil parameters and the detention storage do not vary as a function of grid-cell size. The overland roughness coefficients and channel roughness coefficients are the same as those calibrated for event 1. These results indicate that under more saturated conditions (as is the case for event 2), grid-cell size is less likely to affect the output of the CASC2D

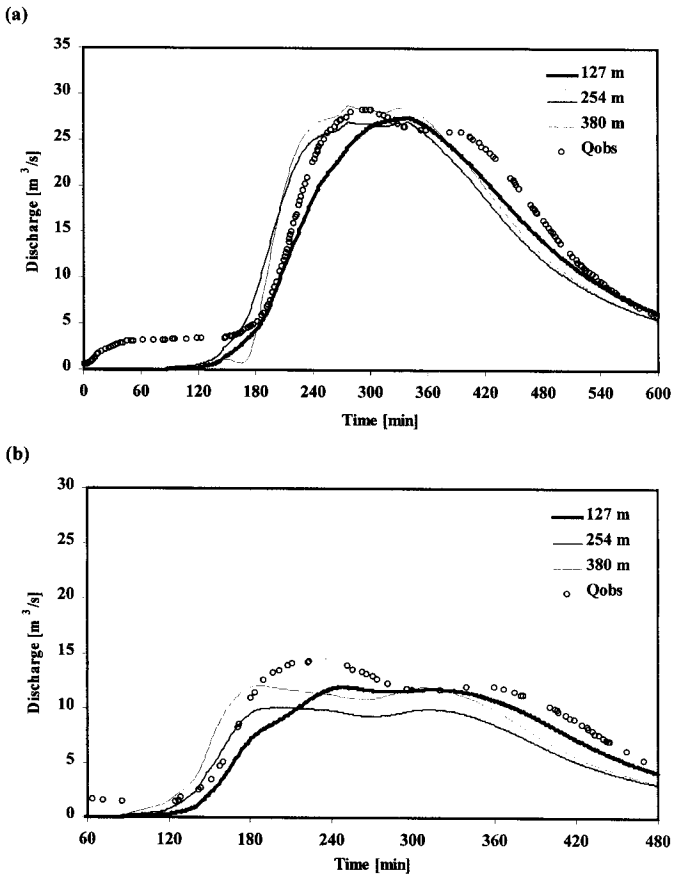

FIG. 2. Goodwin Creek Hydrographs for Event 2: (a) at Outlet; (b) at Gauge 3

TABLE 4. Calibration Parameters for Event 2

Parameter (1)	127 m (2)	254 m (3)	380 m (4)
Overland detention storage S_d (m)	0.00	0.00	0.00
Overland roughness n_{ol}	0.08	0.09	0.15
Silt loam: K_s (m/s)	1.00E-07	1.00E-07	1.00E-07
Silt loam: H_f (m)	0.01	0.01	0.01
Silt loam: M_d	0.0	0.0	0.0
Fine sandy loam: K_s (m/s)	1.50E-07	1.50E-07	1.50E-07
Fine sandy loam: H_f (m)	0.01	0.01	0.01
Fine sandy loam: M_d	0.0	0.0	0.0
Channel roughness n_{ch}	0.037	0.037	0.04

model. Simulated hydrographs at the outlet peak, within 5 min of each other and the discharges, are within 5% of the observed discharge. Hydrographs at the subbasin level were also evaluated, so as to determine the effects of grid-cell size on upland rainfall-runoff processes. The simulated and observed discharges at gauge 3 are presented in Fig. 2(b). All three grid-cell sizes simulate a lower peak discharge. The coarser resolutions result in earlier times-to-peak.

The model validation using event 3 is based on the calibration parameters from event 2, since both events were preceded by significant amounts of rainfall. The rainfall characteristics of event 3 differed significantly from the characteristics of the calibration event. Event 3 lasted five times as long as event 2 and had a total rainfall volume four times the rainfall volume corresponding to event 2. Since CASC2D was used as an event-based model, the rainfall conditions required that an adjustment be made to the initial conditions represented by the detention storage parameter. As a result of the large rainfall volume corresponding to event 3 and its lower rainfall intensity (as compared to event 2), the storage detention parameter S_d was increased from 0.0 to 0.005 at all three grid-cell sizes.

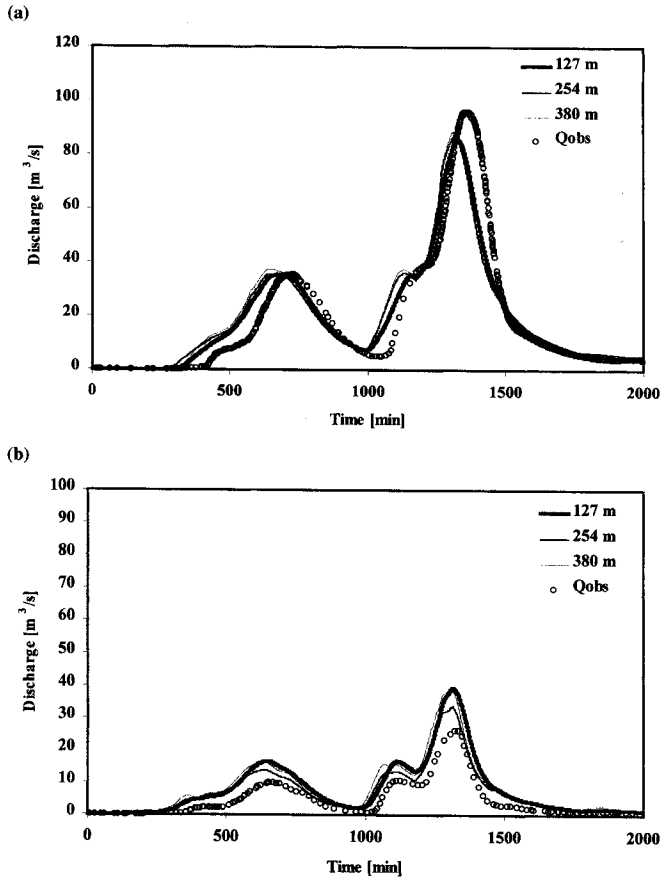

FIG. 3. Goodwin Creek Hydrographs for Event 3: (a) at Outlet; (b) at Gauge 3

The validation runs shown in Fig. 3 produced fairly good agreement between simulated and observed peak discharge rates and time-to-peak at the outlet. The simulated subbasin hydrographs at gauge 3 were also fairly representative of the observed values. For this simulation of 2,000 min the coarser grid size was more appropriate, since it greatly reduced the computation time and yielded similar results to the fine grid-cell size.

EFFECTS OF GRID CELL-SIZE USING DIMENSIONLESS APPROACH

The effects of grid-cell size on the time-to-equilibrium in a watershed can be studied within a GIS environment. The concept of time-to-equilibrium was tested by simulating a rainstorm of constant rainfall intensity and of long enough duration to exceed equilibrium conditions at the outlet of the basin. Since equilibrium conditions were achieved at the outlet, all other grid cells in the basin had also reached equilibrium. At equilibrium, the peak discharge Q_p on each cell was a constant value equal to the equilibrium discharge Q_e. The equilibrium discharge on each cell is equal to the product of rainfall intensity and the drainage area A_d (Woolhiser 1977):

$$Q_e = iA_d \tag{2}$$

Within a raster-based system, watershed characteristics are defined for each grid cell. These characteristics are considered uniform within the cell, and they can be used in calculating the time-to-equilibrium for every pixel within the basin. The time-to-equilibrium is associated with a uniform rainfall intensity i, and is calculated using (1). Two assumptions are made in order to simplify the evaluation of the time-to-equilibrium for individual grid cells. The first assumption is that the average overland roughness coefficient $\bar{n}_{ol}$ and the average slope $\bar{S}$ corresponding to upland areas can be used in calculating time-to-equilibrium. The second assumption is that runoff length L is equal to $A_d^{0.5}$, where A_d is the drainage area. Assuming impervious runoff conditions and a given rainfall intensity i, the time-to-equilibrium T_e for any point in the basin with a drainage area A_d is thus approximated by

$$T_e \cong \left(\frac{\bar{n}_{ol}A_d^{1/2}}{i^{2/3}\bar{S}^{1/2}}\right)^{3/5} \tag{3}$$

As shown in (3), the time-to-equilibrium decreases as rainfall intensity increases. In relation to the drainage area, equilibrium is reached more quickly in upland areas, where A_d values are small, while the longest time-to-equilibrium is associated with the outlet, which drains the largest area.

Analysis on Goodwin Creek

For a given constant uniform rainfall intensity, the time equilibrium T_e can be evaluated for any point in the watershed, using (3), assuming an average Manning overland roughness $\bar{n}_{ol}$, an average upland slope $\bar{S}$, and knowing the drainage area A_d corresponding to that point. If equilibrium discharge Q_e is known, the drainage area can be computed for each cell for a given rainfall intensity, using (2). The theory was tested by assuming impervious conditions on the Goodwin Creek basin, simulating a constant rainfall intensity for a very long duration, and by applying (2) and (3) to each individual grid cell. Since it is known that the outlet of the watershed drains a total area of 21 km^2, for a constant and uniform rainfall intensity of 12.7 mm/h the equilibrium outlet discharge is

$$Q_e = iA_d = 0.000003528*21{,}000{,}000 = 74 \text{ m}^3/\text{s} \tag{4}$$

The time-to-equilibrium at the outlet is calculated assuming an average overland Manning coefficient of 0.08, an average slope of 0.015, and a runoff length of $A_d^{0.5}$:

$$T_e \cong \left(\frac{0.08*21{,}000{,}000^{1/2}}{0.000003528^{2/3}0.015^{1/2}}\right)^{3/5} = 308 \text{ min} = 5 \text{ h } 8 \text{ min} \quad (5)$$

According to (5), a rainstorm with a constant rainfall intensity of 12.7 mm/h and lasting longer than 308 min should result in equilibrium conditions at the outlet and throughout the Goodwin Creek basin.

In order to ensure equilibrium conditions throughout the watershed, a hypothetical rainfall event lasting 15 h with a uniform intensity of 12.7 mm/h was used in simulating impervious runoff. As a consequence of this event, equilibrium conditions calculated from CASC2D were reached throughout the basin. The drainage areas corresponding to the outlet and internal gauges 3, 5, and 12 are approximately 21 km^2, 9 km^2, 4 km^2, and 0.3 km^2, respectively. Since equilibrium has been reached, peak runoff rates are equal to the equilibrium discharge, which was shown in (2) to be a function of the rainfall intensity and the drainage area. Peak discharge at the outlet and gauges 3, 5, and 12 was 66 m^3/s, 27 m^3/s, 15 m^3/s, and 1 m^3/s, respectively.

Simulated equilibrium discharge hydrographs at the outlet and subbasin locations using grid-cell sizes of 254 and 380 m were identical to the results at 127 m. As expected, grid resolution did not affect the nature of the runoff hydrographs under complete equilibrium conditions.

The analysis described in the previous section was performed for the entire basin. Original calculations were performed using a 127 m grid-cell size. Working within a raster-based environment, the maximum discharge at every pixel was recorded for the impervious CASC2D simulation. Since equilibrium had been reached throughout the basin, the peak discharge recorded at each grid corresponded to the equilibrium discharge of the cell. As seen in Fig. 4(b), equilibrium discharge is lower in the upland areas (Q_e < 1 m^3/s) than it is in the channel (100 m^3/s > Q_e > 1 m^3/s). The largest equilibrium discharge occurs at the outlet, which drains the entire basin.

Using GRASS capabilities for data manipulation, the drainage area associated with each pixel was evaluated using (2), based on the raster map of equilibrium discharge and assuming a uniform rainfall intensity of 12.7 mm/h. The raster map depicting drainage area for each individual pixel is presented in Fig. 4(a). This raster map represents 2D routing of overland flow and 1D routing of channel flow, based on the Saint-Venant equations as formulated in CASC2D. Knowing the drainage area associated with each grid cell and the average upland values of the roughness coefficient and slope, the time-to-equilibrium corresponding to a uniform rainfall intensity of 12.7 mm/h was evaluated for every cell by applying (3). The spatial variability of the time-to-equilibrium throughout the basin is shown in Fig. 4(c). The times-to-equilibrium corresponding to individual cells range from 15 min in upland areas to 300 min at the outlet.

The drainage area associated with individual grid cells will always have the same value regardless of rainfall intensity. Equilibrium discharge and time-to-equilibrium will vary as a function of rainfall intensity. Raster maps described A_d, Q_e, and T_e were generated using the techniques described above for a 254 m grid-cell size and a 380 m grid-cell size. Basin-wide values of equilibrium discharge were determined for a 15 h rainfall event of 12.7 mm/h, assuming impervious conditions ($Q_p = Q_e$). Knowing equilibrium discharge, the drainage areas and times-to-equilibrium corresponding to individual cells were calculated using (2) and (3). A comparison of the

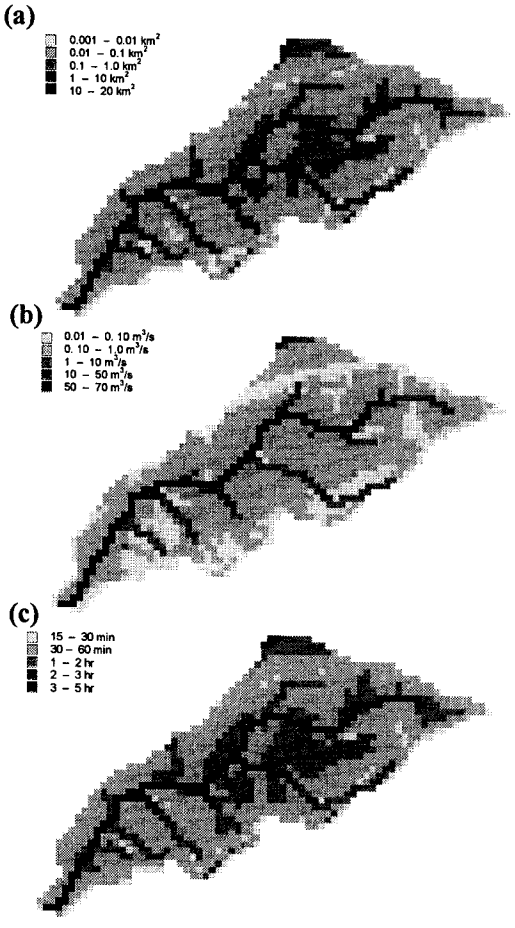

FIG. 4. Spatial Variability on Goodwin Creek: (a) Drainage Area; (b) Equilibrium Discharge; (c) Time-to-Equilibrium

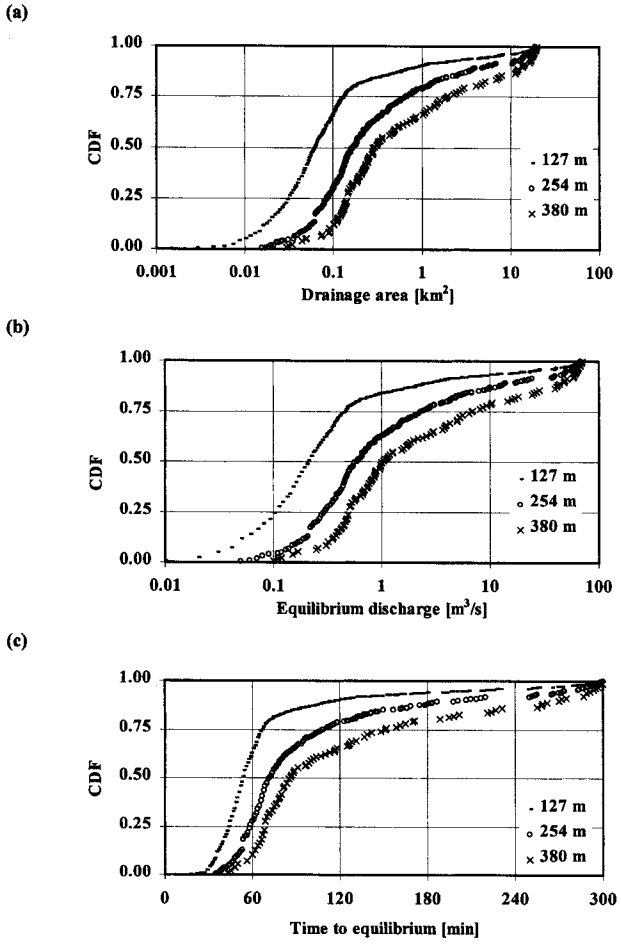

FIG. 5. Goodwin Creek Cumulative Distribution: (a) Drainage Area; (b) Equilibrium Discharge; (c) Time-to-Equilibrium

spatial basinwide distributions of A_d, Q_e, and T_e for the different grid-cell sizes used in the study is presented in Figs. 5(a–c, respectively).

The effect of grid-cell size on the drainage area shown in Fig. 5(a) is to increase the areas associated with individual cells. For instance, for cell sizes of 127, 254, and 380 m, 50% of the cells (CDF = 0.5) drain less than 0.06, 0.2, and 0.3 km^2, respectively. These cells represent upland runoff conditions. Since time-to-equilibrium and equilibrium discharge are directly related to drainage area, similar patterns are seen on Fig. 5(b and c) in the distributions of equilibrium discharge and time-to-equilibrium at increasing grid-cell size. Larger grid-cell sizes result in higher values of drainage areas corresponding to individual cells, and therefore longer times are required before equilibrium is reached, particularly in upland areas. The implication of these results is that coarser grid-cell sizes increase time-to-equilibrium, shifting upland areas toward partial equilibrium. For similar rainfall characteristics, upland areas will take longer to reach equilibrium when coarser grid-cell sizes are used. At the subbasin level, coarse grid cell will be less effective in reproducing observed flow if equilibrium is not reached. If the rainfall event lasts a long time, then equilibrium will be reached in upland areas and the grid-cell size will be irrelevant. In addition to the general effects of grid-cell size on drainage area, time-to-equilibrium, and equilibrium discharge, the results on Goodwin Creek can be used to show the different responses of overland cells and channel cells. As seen in Fig. 6(a), channel drainage patterns are similar at all resolutions, particularly for CDF values greater than 0.50 (toward the outlet of the basin). The results using a 127 m grid-cell size show a clear shift in the nature of the distribution of drainage areas at 1 km^2 [Fig. 6(a)], indicating that 1 km^2 may be a break-off point in describing the spatial variability of watersheds. As seen in Fig. 6(b), in contrast to channel conditions, overland drainage patterns are affected by grid resolution. The coarser resolutions lead to larger drainage areas associated with individual cells. The fine resolution provides a smoother description of overland drainage patterns. It should be noted that drainage areas corresponding to overland cells are never greater than 1 km^2.

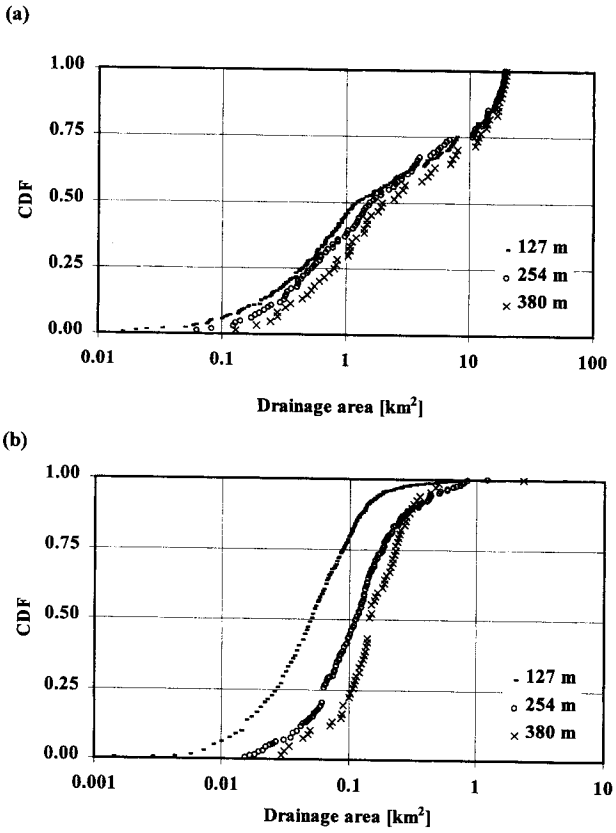

FIG. 6. Goodwin Creek Cumulative Distribution: (a) Channel Cells; (b) Overland Cells

Analysis on Hickahala-Senatobia

The approach used on Goodwin Creek was applied to a larger basin, the Hickahala-Senatobia basin, which drains a total area of 560 km^2. The equilibrium discharge at the outlet of the basin, corresponding to a constant excess rainfall intensity of 12.7 mm/h, is calculated as

$$Q_e = iA_d = 0.000003528 \text{ m/s} * 560{,}000{,}000 \text{ m}^2 = 1{,}976 \text{ m}^3/\text{s} \quad (6)$$

The time-to-equilibrium at the outlet is estimated assuming an average Manning coefficient of 0.08, an average slope of 0.01, and a runoff length equal to $A_d^{0.5}$, such that

$$T_e \cong \left(\frac{0.08 * 560{,}000{,}000^{1/2}}{0.000003528^{2/3} 0.01^{1/2}}\right)^{3/5} = 15 \text{ h } 30 \text{ min} \quad (7)$$

According to (7), a rainstorm with a constant excess rainfall intensity of 12.7 mm/h and lasting longer than 16 h should result in equilibrium conditions at the outlet and throughout the basin.

The total volume of water corresponding to a constant rainstorm intensity of 0.5 in/h, lasting 16 h, would be approximately 10^8 m^3. It was not possible to simulate an event of such a magnitude on Hickahala-Senatobia, nor was the equilibrium outlet discharge of 1,976 m^3/s feasible, given the hydraulic geometry of the channel network. Rather than simulating equilibrium conditions throughout the basin in order to compute drainage area and time-to-equilibrium based on equilibrium discharge, as was the procedure used on Goodwin Creek, an alternative method was applied.

Within GRASS the program *r.watershed* (*Grass 4.1* 1993) uses a digital elevation model (DEM) to evaluate the accumulated number of cells draining to any given cell. Knowing the accumulated number of cells draining to each grid cell, a raster map depicting the drainage area associated with every pixel can be created. This method was used to develop a raster map showing the drainage areas A_d corresponding to individual grid cells in the Hickahala-Senatobia basin. The raster map developed using a 305 m grid-cell size is presented in Fig. 7(a). As seen in that figure, most upland cells have drainage areas less than 1 km^2. Drainage areas corresponding to channel cells range from 10 to 560 km^2.

The equilibrium discharge and the time-to-equilibrium corresponding to a constant rainstorm intensity of 12.7 mm/h were calculated once drainage areas per pixel were determined. Eqs. (2) and (3) were applied to every cell in the basin, assuming a runoff length of $A_d^{0.5}$ and basinwide average values of overland roughness and slope. The raster maps showing the spatial variability of Q_e and T_e are presented in Figs. 7(b and c), respectively. In upland areas, about 75% of the grid cells have equilibrium runoff rates less than 10 m^3/s and times-to-equilibrium less than 4 h. Within the channel network, equilibrium runoff rates exceed 100 m^3/s and times-to-equilibrium are greater than 6 h.

The analysis was repeated using a 610 m and a 914 m grid-cell size. The drainage areas corresponding to each grid cell were evaluated using the GRASS program *r.watershed*. Equilibrium discharge and time-to-equilibrium for individual cells were then calculated, assuming a constant rainfall intensity of 12.7 mm/h. Comparisons of the spatial basinwide distributions of A_d, Q_e, and T_e are presented in Figs. 8(a–c), respectively. As seen in the results, the smallest drainage area at each grid-cell size corresponds to the drainage area of a single cell. Cells with drainage areas less than 10 km^2 are overland cells.

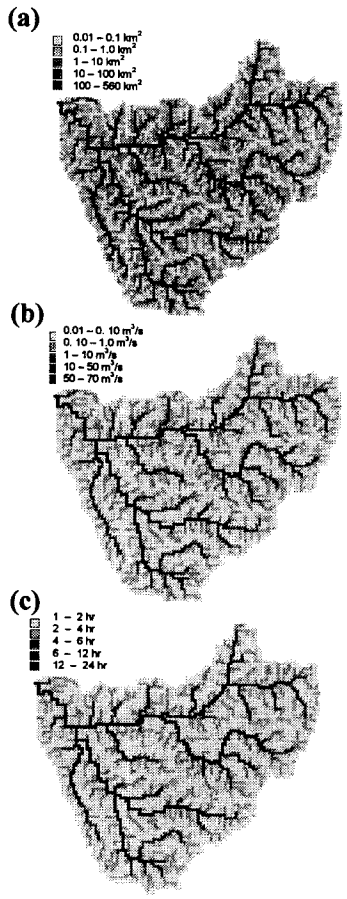

FIG. 7. Spatial Variability on Hickahala: (a) Drainage Area; (b) Equilibrium Discharge; (c) Time-to-Equilibrium

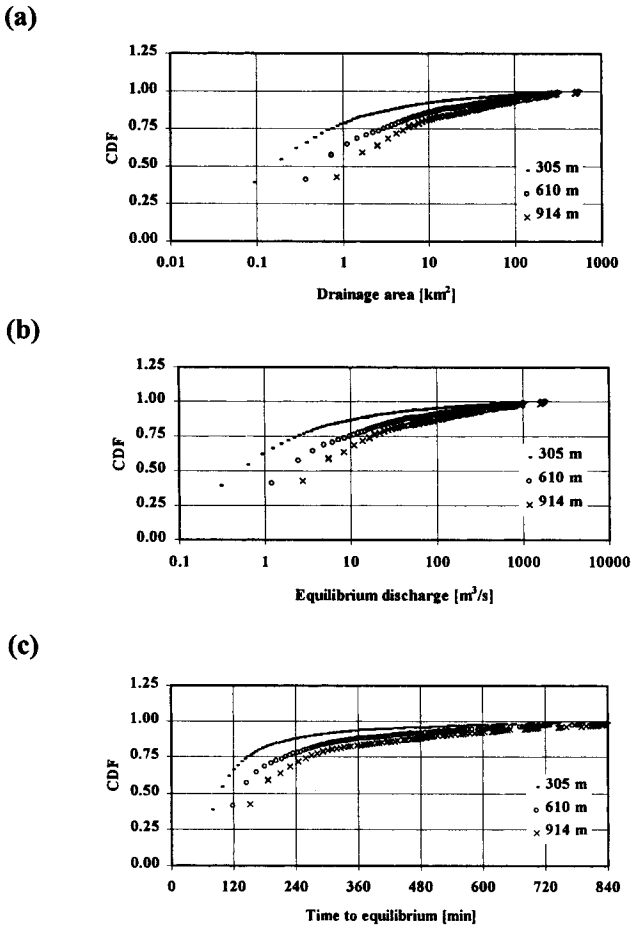

FIG. 8. Hickahala Cumulative Distribution: (a) Drainage Area; (b) Equilibrium Discharge; (c) Time-to-Equilibrium

According to the results on Hickahala-Senatobia, trends shown to occur on large watersheds are similar to those seen on small watersheds. Grid-cell primarily affects runoff conditions on overland cells. These results indicate that if rainfall characteristics are such that it is expected that only partial equilibrium will be reached in upland areas, then smaller grid cells should be used. If an event lasts a long time or is of high intensity, then equilibrium conditions will be met throughout most of the watershed and coarser grid-cell sizes can be used in distributed rainfall-runoff modeling.

CONCLUSIONS

Analyses on Goodwin Creek show that the CASC2D model can be used in simulating observed peak discharge and time-to-peak at the outlet, using grid-cell sizes ranging up to 380 m, as long as the model is calibrated at the given grid-cell size. The model CASC2D is capable of reproducing observed discharge both at the outlet and at the subbasin level. Even the coarsest resolution led to fairly accurate estimates of the peak magnitude and the time-to-peak corresponding to a given rainfall event. The primary effect of increasing grid-cell size is to require higher overland and channel roughness coefficients, as shown in Tables 3 and 4. This increase is related to the representation of watershed characteristics influencing overland and channel flow. In addition, according to simulations results, when initial soil moisture is high, soil and detention storage parameters are not affected by grid-cell size (Table 4). These results indicate (Figs. 2 and 3) that grid resolution will have less of an effect on runoff simulations if the soil is saturated at the beginning of the event.

The effects of grid size on excess rainfall generation and routing processes using the concept of a watershed time-to-equilibrium were examined on Goodwin Creek and Hickahala-Senatobia using a GIS-GRASS database. The results indicate that as grid-cell size increases, the time-to-equilibrium in upland cells also increases, since the drainage areas corresponding to individual grid cells increase. The distributions of drainage area corresponding to overland cells are most sensitive to changes in grid-cell size, whereas channel cells are hardly affected by grid-cell size. At the outlet and throughout the channel network, equilibrium conditions are constant because the drainage areas corresponding to these points do not change. The distribution of drainage areas subsequently affects the distribution of the time-to-equilibrium basinwide.

Selecting an appropriate grid-cell size is particularly important when the rainfall event is of a short duration and equilibrium conditions are likely not to be met. In this case the nature of the runoff hydrograph is greatly influenced by physical basin characteristics, the variability of which may not be represented by coarse grid cells. Smaller grid-cell sizes should be used for short storms so as to reach equilibrium in upland areas. When long rainfall events are simulated, larger grid-cell sizes can be used, since equilibrium will be reached throughout most of the upland areas. These conclusions regarding grid size are consistent with results published by Julien and Moglen (1990).

Results from this study indicate that the applicability of the distributed hydrologic model CASC2D can be extended to watershed greater than 500 km^2, and that large grid-cell sizes can be used without sacrificing important information on the spatial variability of the processes affecting surface runoff. The larger grid-cell sizes will be particularly useful in simulating events on large watersheds, since they require less-detailed input data and result in much shorter computation times. Coarser cells will also be more applicable when initial soil

moisture conditions are saturated, but roughness coefficients may have to be modified.

ACKNOWLEDGMENTS

The writers would like to thank B. E. Johnson, C. Downer, and J. Jorgeson at Waterways Experiment Station for their contributions in the data acquisition process. We would also like to thank C. Alonso and R. Bingner at ARS in Oxford, Mississippi for providing information on Goodwin Creek. The writers would also like to thank peer reviewers for their helpful comments.

APPENDIX I. REFERENCES

Agiralioglu, N. (1988). "Estimation of the time of concentration for diverging surfaces." *J. Hydrolog. Sci.*, 33(2), 173–179.

Beven, K. (1983). "Surface water hydrology: Runoff generation and basin structure." *Rev. of Geophys.*, 21(3), 721–729.

Blackmarr, W. A., Ed. (1995). "Documentation of hydrologic, geomorphic, and sediment transport measurements on Goodwin Creek experimental watershed, Northern Mississippi, for the period 1982–1993—preliminary release." Agricultural Research Serv., U.S. Dept. of Agriculture, Oxford, Miss., 141.

Doe, W. W., and Saghafian, B. (1992). "Spatial and temporal effects of army maneuvers on watershed response: The integration of GRASS and a 2-D hydrologic model." *Proc., 7th Annu. GRASS Users Conf., Tech. Rep. NPS/NRG15D/NRTR-93/13*, National Park Service, Lakewood, Colo., 91–165.

Dunne, T. (1982). "Models of runoff processes and their significance." *Scientific Basis of water resource management*, National Academy Press, Washington, D.C., 17–30.

GRASS 4.1 user's reference manual. (1993). USACE, Compiled at Construction Engineering Research Labs., Champaign, Ill., 458.

Henderson, F. M., and Wooding, R. A. (1964). "Overland and groundwater flow from a steady rainfall of finite duration." *J. Geophys. Res.*, 69(8), 1531–1540.

James, L. D., and Burges, S. J. (1982). "Selection, calibration, and testing of hydrologic models." *Hydrological modeling of small watersheds*, C. T. Haan, H. P. Johnson, and D. L. Brakensiek, eds., American Society of Agricultural Engineers, St. Joseph, Mich., Monogr. Ser., 5, 435–472.

Johnson, B. E. (1993). "Comparison of distributed vs. lumped rainfall-runoff modeling techniques," MS thesis, Memphis State University, Memphis, Tenn.

Johnson, B. E., Raphelt, N. K., and Willis, J. C. (1993). "Verification of hydrologic modeling systems." *Proc., Federal Water Agency Workshop on Hydrologic Modeling Demands for the 90's, Rep. 93-4018*, Water Resources Investigations, U.S. Geological Survey, Sec. 8., 9–10.

Julien, P. Y., and Moglen, G. E. (1990). "Similarity and length scale for spatially varied overland flow." *Water Resour. Res.*, 26, 1819–1832.

Julien, P. Y., Saghafian, B., and Ogden, F. L. (1995). "Raster-based hydrological modeling of spatially-varied surface runoff." *Water Resour. Res.*, 31(3), 523–535.

Lighthill, M. H., and Whitham, G. B. (1955). "On kinetic waves, I: Flood movement in long rivers." *Proc., Royal Society of London*, Ser. A, 229, 281–316.

Molnár, D. K. (1997). "Grid size selection for 2-D hydrologic modeling of large watersheds," PhD dissertation, Colorado State University, Ft. Collins, Colo.

Ogden, F. (1992). "Two-dimensional runoff modeling with weather radar data," PhD dissertation, Colorado State University, Ft. Collins, Colo.

Ogden, F., and Julien, P. Y. (1994). "Two-dimensional runoff sensitivity to radar resolution." *J. Hydrol.*, 128(1–2), 1–18.

Ogden, F., Richardson, J. R., and Julien, P. Y. (1995). "Similarity in catchment response. 2: Moving rainstorms." *Water Resour. Res.*, 31(6), 1543–1547.

Rawls, W. J., Brakensiek, D. L., and Miller, N. (1983). "Green-Ampt infiltration parameters from soils data." *J. Hydr. Engrg.*, ASCE, 109(1), 62–70.

Saghafian, B. (1992). "Hydrologic analysis of watershed response to spatially varied infiltration," PhD dissertation, Colorado State University, Ft. Collins, Colo.

Saghafian, B., and Julien, P. Y. (1995). "Time to equilibrium for spatially variable watersheds." *J. Hydrol.*, 172, 231–245.

Saghafian, B., Julien, P. Y., and Ogden, F. L. (1995). "Similarity in catchment response, 1: Stationary rainstorms." *Water Resour. Res.*, 31(6), 1533–1541.

Sivapalan, M., Beven, K., and Wood, H. F. (1987). "On hydrologic similarity, 2: A scaled model of storm runoff production." *Water Resour. Res.*, 23(12), 2266–2278.

Wood, E. F. (1983). "Hydrology 1979–1982." *Rev. of Geophys.*, 21(3), 697–698.

Wood, E. F., Sivapalan, M., Beven, K., and Band, L. (1988). "Effects of spatial variability and scale with implications to hydrologic modeling." *J. Hydrol.*, 102, 29–47.

Wood, E. F., Sivapalan, M., and Beven, K. J. (1990). "Similarity and scale in catchment storm response." *Rev. of Geophys.*, 28(1).

Wooding, R. A. (1965a). "A hydraulic model for the catchment-stream problem, I. Kinematic-wave theory." *J. Hydrol.*, 3, 254–267.

Wooding, R. A. (1965b). "A hydraulic model for the catchment-stream problem, II. Numerical solutions." *J. Hydrol.*, 3, 268–282.

Wooding, R. A. (1966). "A hydraulic model for the catchment-stream problem, III. Comparison with runoff observations." *J. Hydrol.*, 4, 21–37.

Woolhiser, D. A. (1975). "Simulation of unsteady overland flow." *Unsteady flow in open channels*, K. Mahmood and V. Yevjevich, eds., Vol. II, Water Resource Publ., Ft. Collins, Colo.

Woolhiser, D. A. (1977). "Unsteady free-surface flow problems." *Mathematical models for surface water hydrology*, Wiley, New York, 195–213.

Woolhiser, D. A., and Goodrich, D. (1988). "Effect of storm rainfall intensity patterns on surface runoff." *J. Hydrol.*, 102, 335–354.

APPENDIX II. NOTATION

The following symbols are used in this paper:

A_d = drainage area;
H_f = capillary pressure head;
i = rainfall intensity;
K_s = saturated hydraulic conductivity;
L = runoff length;
M_d = soil moisture deficit;
n = Manning roughness coefficient;
n_{ol} = overland Manning roughness coefficient;
n_{ch} = channel Manning roughness coefficient;
$\bar{n}_{ol}$ = average overland roughness coefficient;
Q_e = time-to-equilibrium;
Q_p = peak discharge;
S = runoff slope;
S_d = detention storage;
$\bar{S}$ = average runoff slope;
T_e = time-to-equilibrium; and
T_r = rainfall duration.